Dynamic Analysis of Chemical Relaxation Effects: A Study of Salicylate-Indicator Systems by a T-Jump Apparatus with Laser Monitoring

R. Maggini, F. Secco,* and M. Venturini

Department of Chemistry, University of Pisa, Via Risorgimento 35, 56127 Pisa, Italy

Received: March 6, 1997[⊗]

The kinetics and equilibria of proton-transfer reactions involving 3,5-dinitrosalycilate ion (DNSA) and the indicators Bromothymol Blue (BTB), Thymol Blue (TB), and Phenol Red (PR) have been investigated at ionic strength 0.1 M by a T-jump technique where a system of lasers was employed for monitoring the relaxation effects. The reacting systems display biexponential curves that have been analyzed in terms of *normal reactions*. A method is presented that leads to a quick evaluation of the stoichiometric coefficients of the species taking part in the normal modes of reaction. The kinetic results show that the rates of proton exchange are lower than those of proton recombination by about 3 orders of magnitude, thus indicating that a strong intramolecular hydrogen bond is present in DNSA. The shapes of the plots of log k vs ΔpK suggest that a two-step mechanism involving a fast preequilibrium between a closed (unreactive) and an open (reactive) form of DNSA should be preferred to the one-step mechanism where the acceptor is able to react also with the proton of the closed DNSA. The analysis of the relaxation amplitudes allowed $\Delta G°$ and $\Delta H°$ of the individual steps to be simultaneously evaluated. A comparison between the performance of the T-jump with conventional lamp and that of the T-jump with laser monitoring is in favor of the latter technique, which, in turn, has been demonstrated to be as accurate and precise as classical spectrophotometry.

Introduction

We report here on a T-jump study of proton-transfer reaction between 3,5-dinitrosalicylate monoanion and indicators of the sulfonephtalein family.

The scope of this investigation is 3-fold. First, it lies in the framework of our investigations on the role of internal hydrogen bonds in chemical reactivity.[1−5] The transfer of protons engaged in internal H-bonds can occur by a two-step[6] or by a one-step[7] mechanism, and concerning salicylates, it is not clear, so far, which of them is operative.

The second purpose of this investigation is to present an analysis of the relaxation effects in terms of normal modes according to a mathematical procedure that allows the kinetic and thermodynamic parameters of coupled individual reactions to be easily evaluated.

The third aim of the paper is to show that the signal improvement of the T-jump apparatus with laser detection allows the $\Delta G°$ and $\Delta H°$ of individual reaction steps to be simultaneously determined through the analysis of amplitudes with a precision much higher than that provided by T-jump apparatuses with conventional detection and comparable with that of static methods.

Experimental Section

Materials. All chemicals were analytical grade. Doubly distilled water was used to prepare the stock solutions of the reactants and as a reaction medium. In the following, the reactants will be indicated in short as DNSA (3,5-dinitrosalycilate ion), PR (Phenol Red), BTB (Bromothymol Blue), and TB (Thymol Blue).

Measurements. The measurements of pH were performed by a Radiometer pHM 84 instrument equipped with a combined glass electrode. The usual KCl bridge was replaced by a 3 M NaCl bridge in order to avoid precipitation of $KClO_4$ since sodium perchlorate was added to the reaction mixture in order to keep the ionic strength at the value of 0.1 M. The output of the pH meter was converted to $-\mathrm{Log}[H^+]$ by an already-described procedure.[3] Spectrophotometric titrations were performed with a Perkin-Elmer Lambda UV17 spectrophotometer. Known amounts of $HClO_4$ were added by an Agla microsyringe directly into the spectrophotometric cell containing a known excess of buffer (K_2HPO_4 or NH_3) and the alkaline form of the indicator.

The DNSA/TB system was studied by using a T-jump instrument manufactured by Messanlagen mbH (Gîttingen), whereas the DNSA/BTB and DNSA/PR systems were investigated by a T-jump apparatus devised in our department that makes use of lasers as detection light sources.[8] The advantage of this instrument relies on the fact that it provides a signal-to-noise ratio much more favorable than that of the conventional apparatus, thus allowing fast transient signals of small amplitude to be satisfactorily analyzed. The samples were brought to the desired pH values by small additions of NaOH or $HClO_4$ and then transferred to the T-jump cell, which was thermostated at 22.5 °C. The discharge of a capacitor provided an increase of temperature of 2.5 °C in ca. 4 μs. The signals were acquired by a Datalab DL910 transient recorder that was able to record 4096 data points at a maximum sampling rate of 20 MHz and then sent to an oscilloscope for visualization and to a personal computer for evaluation. A nonlinear least-squares procedure developed by Provencher[9] was used to analyze the relaxation curves as sums of exponentials. The relaxation times and amplitudes were averaged over at least four replicated runs. A general nonlinear regression program developed by Meites[10] was used for the evaluation of the rate constants.

Results

Equilibria. Owing to remarkable structural similarities, the absorption spectra of the three indicators are similar. Their alkaline forms exhibit intense absorption bands with maxima at 559 nm (PR), 593 nm (TB), and 616 nm (BTB). On the

[⊗] Abstract published in *Advance ACS Abstracts,* July 1, 1997.

S1089-5639(97)00872-4 CCC: $14.00 © 1997 American Chemical Society

TABLE 1: Acid Dissociation Constants and Extinction Coefficient Differences of 3,5-Dinitrosalicylate Ion, Bromothymol Blue, Phenol Red, and Thymol Blue (T = 25 °C, I = 0.1 M ($NaClO_4$))

acid	λ, nm	$10^{-4}\Delta\epsilon$,[a] $M^{-1}cm^{-1}$	pK_A
$H_2PO_4^-$			6.71[b]
NH_4^+			9.29[c]
DNSA	410		7.12 ± 0.02
BTB	633	−3.61	7.08 ± 0.05
			(7.08 ± 0.03)[d]
PR	543	−4.97	7.70 ± 0.01
TB	585	−3.34	8.85 ± 0.01
			(8.81 ± 0.19)[d]

[a] $\Delta\epsilon = \epsilon_{Hin} - \epsilon_{In}$. [b] Reference 13. [c] Reference 14. [d] From relaxation amplitudes.

other hand, DNSA does not absorb at wavelengths above 510 nm. The acid dissociation constants of DNSA, PR, BTB, and TB were obtained spectrophotometrically by measuring the equilibrium constant of reaction 1

$$HIn^- + B \rightleftharpoons In^{2-} + HB \quad (1)$$

where B designates HPO_4^{2-} ion or NH_3. The analytical concentrations of buffer and indicator were, respectively, $C_B = 2 \times 10^{-3}$ M and $C_{In} = 2 \times 10^{-5}$ M in most experiments. Introduction of the mass conservation for the indicator and the expression for the equilibrium constant of reaction 1 in the Lambert−Beer law leads to

$$C_{In}/\Delta A = 1/\Delta\epsilon + 1/(K\Delta\epsilon)[HB]/[B] \quad (2)$$

where A is the absorbance, $\Delta A = A - \epsilon_{Hin}C_{in}$, $\Delta\epsilon = \epsilon_{In} - \epsilon_{Hin}$, and K is the equilibrium constant of reaction 1. The titrations were performed under the conditions $C_B \gg C_{In}$. Therefore, $[HB]/[B] = C_{HClO_4}/(C_B - C_{HClO_4})$, where C_{HClO_4} indicates the concentration of the added perchloric acid. The data, plotted according to eq 2, yield good linear plots that allow the evaluation of $\Delta\epsilon$ and K. The acid dissociation constants of the indicators were then evaluated from the relationship $pK_{HIn} = pK + pK_{HB}$.

The same procedure was employed to evaluate the acid dissociation constant of DNSA (buffer phosphate, $\lambda = 410$ nm). The results of the spectrophotometric measurements are collected in Table 1. Some titrations of mixtures of indicator and DNSA were performed for the sake of comparison in the case of BTB and PR. The values of K are in excellent agreement with those evaluated from the data of Table 1.

The equilibrium constants of reaction 1 were measured at different temperatures for each indicator. Their values were used to draw Van't Hoff plots whose slopes yielded the $\Delta H°$ values quoted in parentheses in Table 3.

Kinetics. All kinetic experiments have been performed in the absence of buffer. The process of proton transfer is appropriately described by eqs A1−A6 of the Appendix, which include a set of six coupled steps, three of them being thermodynamically independent. The reciprocal of the three relaxation times that in principle characterize the dynamic behavior of the system depend on the concentration variables according to the third-degree eq A14. However, if $H^+$and OH^- be present in small amounts compared to the other components, eq A11 is reduced to a first-degree equation, which can be put in the form[3,11]

$$\lambda = (\text{exch} + \text{prot} + \text{hydr})F \quad (3)$$

where exch = k_2, prot = $K_{HL}/([In^{2-}]/k_1 + [L^{2-}]/k_4)$, hydr = $(K_W/K_{HIn})/([HIn^-]/k_6 + [HL^-]/k_3)$, and $F = [HL^-] + [In^{2-}] + (K_{HIn}/K_{HL})([L^{2-}] + [HIn^-])$. L^{2-} and HL^- denote, respectively, the unprotonated and the monoprotonated DNSA. The parameters $k_1...k_6$ represent the second-order rate constants, in the forward direction, of steps $A_1...A_6$, respectively.

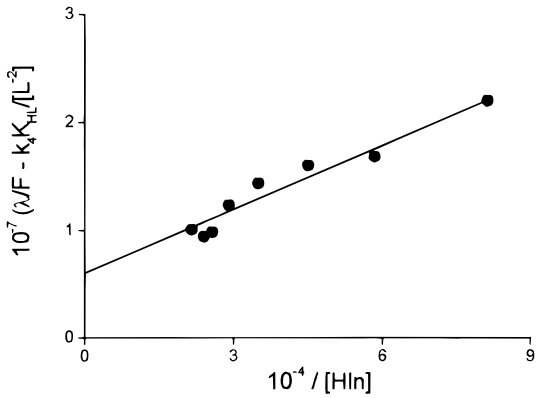

Figure 1. DNSA/TB system. Graphical analysis of the relaxation times. 8.1≤ pH ≤ 9.1, T = 25 °C, I = 0.1 M, λ = 585 nm.

The TB/DNSA System. All measurements were carried out at λ = 585 nm (tungsten lamp monitoring). The DNSA concentration, C_L, was changed from 5×10^{-4} to 2×10^{-3} M, whereas that of the indicator, C_{In}, never exceeded the value of 5×10^{-5} M. The pH of the solutions was changed between 7.5 and 9.3. The relaxation curves were composed of two exponential effects with amplitudes of opposite sign. Owing to unfavorable signal-to-noise ratio, the fastest effect could not be analyzed. The relaxation time of the slowest effect changes with pH on going through a minimum, meaning that each of the three terms of eq 3 makes a contribution to the overall process. Figure 1 shows a graphical analysis of the data between pH 8.1 and 9.3 where the contribution of the protolysis path is less important than at the higher acidities. In addition, under these circumstances, the inequalities $[In^{2-}]/k_1 \ll [L^{2-}]/k_4$ and $[HL^-]/k_3 \ll [HIn^-]/k_6$ hold. Equation 3 is then reduced to

$$\frac{\lambda}{F} - \frac{K_{HL}k_4}{[L^{2-}]} = k_2 + \frac{K_W k_6}{K_{HIn}[HIn^-]} \quad (4)$$

By using the Debye equation[12] with a distance of closest approach[11] of 8×10^{-8} cm, we calculated $k_4 = 4 \times 10^{10}$ M^{-1} s^{-1}. The intercept and slope of the linear plot drawn according to eq 4 yield, respectively $k_2 = 6.0 \times 10^6$ M^{-1} s^{-1} and $k_6 = 1.8 \times 10^7$ M^{-1} s^{-1}. A nonlinear least-squares analysis was then performed over the full set of data according to both eq 3 and eq A14 with very similar results. In order to reduce the number of parameters to be evaluated, the constraints $k_1 = k_4$ and $k_6 = 3k_2$ were introduced. The first is justified by the fact that steps A1 and A4 both refer to proton recombination and therefore are diffusion controlled. The second is justified by the results of the graphical analysis shown in Figure 1. The values of the rate constants are given in Table 2.

The DNSA/PR System. All measurements were performed at 543 nm (laser monitoring). The DNSA concentration was $(0.5-2) \times 10^{-3}$ M in larger excess over the indicator concentration, which was $(2-7) \times 10^{-5}$ M. The pH was varied between 7.3 and 8.6. Here too, the experiments revealed the presence of two relaxation effects, but in this case, thanks to much higher light intensity, the signal-to-noise ratio was very favorable,[8] and it was possible to evaluate the full curve. A typical experiment is shown in Figure 2 where the continuous line has been calculated according to two exponentials.

The analysis of the relaxation times was performed according to eq A14, and the values of the kinetic parameters are collected in Table 2.

TABLE 2: Rate Constants (M^{-1} s^{-1}) for the Proton-Transfer Process between DNSA and Indicators (I = 0.1 M ($NaClO_4$), T = 25 °C)

	donors				
	H^+	$HDNSA^-$	$HBTB^-$	HPR^-	HTB^-
OH^-	1.4×10^{11}	2.4×10^7 (1.8×10^7)[a]			3.0×10^{10}
$DNSA^{2-}$	6.8×10^{10}		9.7×10^6	2.6×10^6	1.1×10^5
BTB^{2-}	3.3×10^{10}	8.7×10^6			
PR^{2-}	8.5×10^{10}	9.6×10^6			
TB^{2-}	8.5×10^{10}	5.6×10^6 (6.0×10^6)			
H_2O[b]		5.2×10^3	2.7×10^3	1.7×10^3	1.3×10^2

[a] The values in parentheses have been obtained from the plot of Figure 2. [b] The rate constants are in s^{-1}.

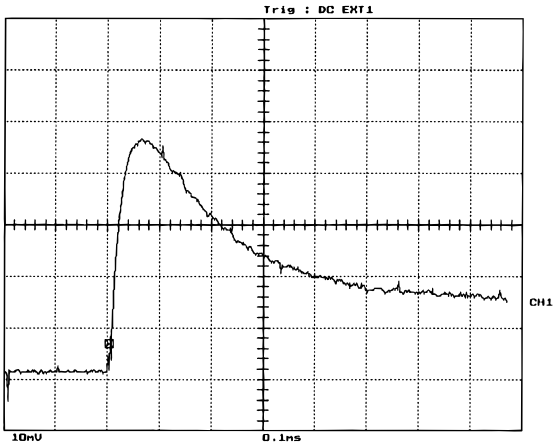

Figure 2. Diexponential relaxation effect for the DNSA/PR system monitored with a 0.5 mW laser as light source. The signal is proportional to the light intensity. T = 25 °C, δT = 2.5 °C, I = 0.1 M, λ = 543 nm, rise time = 2 μs, heating time = 4 μs, pretrigger = 0.2 ms.

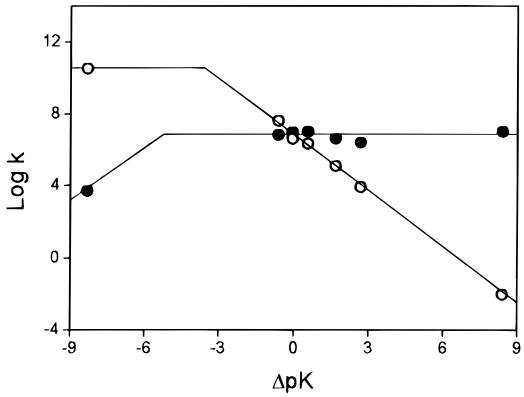

Figure 3. Plot of log k vs ΔpK for the proton-exchange reaction between DNSA and different acceptors. T = 25 °C, I = 0.1−0.3 M. Acceptors (from left to right): H_2O, cacodylate (ref 3), BTB, PR, TB, NH_3 (ref 3), OH^-.

The DNSA/BTB System. All measurements were performed at 633 nm (laser monitoring). The DNSA concentration was (0.5−1.5) × 10^{-3} M and that of the indicator (1−3) × 10^{-5} M, whereas the pH was varied between 6.5 and 7.9. A single exponential curve of negative amplitude was observed in most cases, but some experiments, carried out at pH ≥ 7.8, revealed the presence of a second exponential of positive amplitude. The relaxation times, analyzed according to eq A14, yielded the rate constants collected in Table 2.

Figure 3 shows plots of the logarithms of the rate constants for proton-transfer reactions between DNSA and acceptors/donors of different basicity *vs* ΔpK ($pK_{HIn} - pK_{HL}$).

Relaxation Amplitudes. The amplitudes of the relaxation effects should be associated, rather than to the individual steps, to special linear combinations of them denoted as *normal modes of reaction* or more simply *normal* reactions.[1] The amplitude of the kth normal reaction, expressed as a change of absorbance, δA_k, following a jump of temperature δT, is related to the relevant thermodynamic parameters by the relationship[15−19]

$$\delta A_k = \Gamma_k \Delta\epsilon_k \Delta H^\circ_k \delta T / RT^2 \qquad (5)$$

where $\Gamma_k = (\Sigma N_{ik}^2/c_i)^{-1}$ is the amplitude factor whose magnitude depends on the stoichiometric coefficients N_{ik} and on the equilibrium concentrations, c_i, of the species taking part in the kth normal reaction.[1] $\Delta\epsilon_k$ is the extinction coefficient difference, and ΔH_k° is the reaction enthalpy.

The normal reactions are given in the form A15. The first normal reaction (k = 1) is too fast to be observed by the T-jump method on the basis of discharge of a capacitor. Moreover, the evaluation of the coefficients C_{jk}, according to eq A13, shows that for the second (k = 2) and third (k = 3) normal reaction the terms (C_{1k}/C_{3k}) are always negligible. Therefore, the two normal reactions associated to the observed amplitudes will take the form

$$(C_{2k}/C_{3k})\mathrm{A2} + \mathrm{A3} \qquad (k = 2, 3) \qquad (6)$$

or, more explicitly

$$(C_{2k}/C_{3k})HL^- + (C_{2k}/C_{3k} - 1)In^{2-} + OH^- = (C_{2k}/C_{3k})L^{2-} + (C_{2k}/C_{3k} - 1)HIn^- + H_2O \qquad (6a)$$

Obviously, the same linear combination will hold for the physicochemical properties of the normal reactions, namely

$$\Delta\epsilon_k = (C_{2k}/C_{3k})\Delta\epsilon_{A2} + \Delta\epsilon_{A3} \qquad (7)$$

$$\Delta H^\circ_k = (C_{2k}/C_{3k})\Delta H^\circ_{A2} + \Delta H^\circ_{A3} \qquad (8)$$

The DNSA/PR System. The coefficients C_{jk} for this system range within the intervals $0.033 \le C_{22}/C_{32} \le 0.1$ and $3 \le C_{23}/C_{33} \le 30$. The ranges of variability are well separated; therefore, the two normal reactions cannot degenerate into a single normal mode. On the other hand, none of the factors of eq 5 becomes so small to suppress either of the two amplitudes. Therefore, the system should display two relaxation effects through the full range of concentrations as experimentally observed. The fastest of the two exponential effects shown in Figure 2 is associated to the second normal reaction (k = 2). Its amplitude is negative. The experimental conditions are such that (C_{22}/C_{32}) is so small that in most of the experiments the contribution of step A2 to the normal reaction (6) could be neglected. Therefore, the fast normal reaction (k = 2) is reduced to the hydrolysis step A3. The reaction enthalpy of reaction A3 has been evaluated by introducing the measured amplitudes in eq 5. Its value, averaged over 25 experiments, is given in Table 3.

The slowest of the two effects is associated to the third normal reaction (k = 3). Here, the magnitude of C_{23}/C_{33} is such that the contribution of step A2 to the normal reaction (6) could not be neglected. The reaction enthalpy of this normal mode depends linearly on C_{23}/C_{33} according to eq 8 as shown in Figure 4. The slope and intercept of the straight line yield the reaction enthalpies of the proton exchange step A2 and of the hydrolysis step A3, respectively, whose values are collected in Table 3.

The DNSA/BTB System. The analysis of the amplitudes has been restricted to the experiments performed below pH 7.1

TABLE 3: Reaction Enthalpies (KJ mol^{-1}) for the Different Steps Contributing to the Process of Proton Transfer in the DNSA/Indicator Systems (I = 0.1 M ($NaClO_4$), T = 25 °C)

	$HL^- + In^{2-} \rightleftharpoons HIn^- + L^{2-}$	$H^+ + In^{2-} \rightleftharpoons HIn^-$	$OH^- + HIn^- \rightleftharpoons In^{2-} + H_2O$
BTB	7.19 ± 0.67	−4.93	−51.1
	(7.52 ± 0.38)[a]		
PR	−2.76 ± 0.25	−14.9	−41.1
	(−2.68 ± 0.29)		−42.6 ± 2.7[b]
TB	−6.52 ± 1.5	−18.6	−37.4
	(−6.60 ± 0.17)		

[a] All values in parentheses have been derived from static titrations at different temperatures. [b] From the analysis of the amplitudes of normal reaction II.

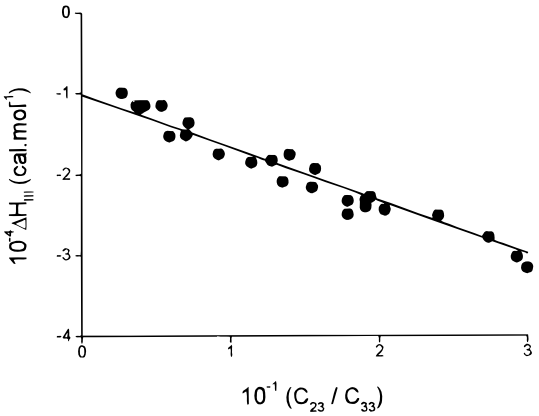

Figure 4. Dependence of the reaction enthalpy of the third normal reaction, ΔH_{III}, on the ratio C_{23}/C_{33} for the DNSA/PR system. T = 25 °C, I = 0.1 M.

where only a single relaxation effect ascribable to the third normal reaction (k = 3) was measured. It has been found that $C_{23}/C_{33} \gg 1$ for all experiments. Therefore, the third normal mode practically coincides with the proton-exchange reaction A2. Under these circumstances, eq 5 can be put in the form of eq 9

$$\left(\frac{C\mathrm{In}[H^+]}{\delta A}\right)^{1/2} = \left(\frac{K_{HIn}RT^2}{\Delta\epsilon\Delta H^\circ\delta T}\right)^{1/2} + \left(\frac{RT^2}{K_{HIn}\Delta\epsilon\Delta H^\circ\delta T}\right)^{1/2}[H^+] \quad (9)$$

which allows the dissociation constant of the indicator and the reaction enthalpy of the proton-exchange step to be simultaneously evaluated from the plot shown in Figure 5.

The acid dissociation constant of BTB is reported as pK_{HIn} in Table 1, whereas the reaction enthalpy of the proton-exchange step A2 is reported in Table 3. Deviations from linearity are shown at pH values higher than 7.2. This is due to the fact that under these conditions the inequality $C_{23}/C_{33} \gg 1$ does not hold anymore and a contribution from the hydrolysis step makes itself felt.

The DNSA/TB System. The analysis of the amplitudes was performed according to eq 9 since $C_{23}/C_{33} \gg 1$ in this case also. The values of K_{HIn} and ΔH° of the proton-exchange step A2 were obtained from a plot similar to that of Figure 5 and are given in Tables 1 and 3, respectively.

Discussion

Static Measurements. The dissociation constants of the three indicators are in good agreement with the literature data.[20] Their values change in the order BTB > PR > TB, reflecting the electronic effects of the substituents on the rates of proton dissociation k_{-4}.

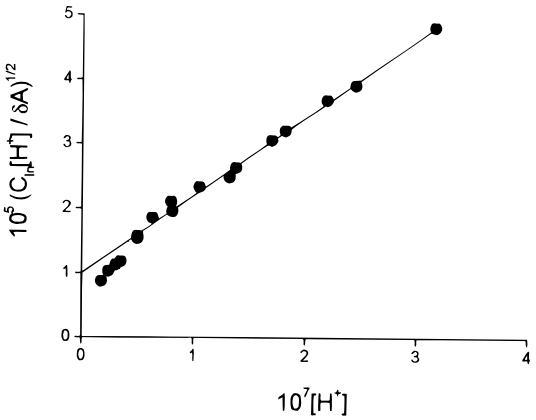

Figure 5. Analysis of the amplitudes of the DNSA/BTB system. The acid dissociation constant of the indicator and ΔH° of the proton-exchange step are evaluated from slope and intercept of the linear fit. T = 25 °C, I = 0.1 M.

Dynamic Measurements. Table 2 shows that the rate constants for recombination of H^+ with the different acceptors are close together and of the order of magnitude expected for diffusion-controlled reactions.[11] The rate constants for proton transfer from $HDNSA^-$ to the indicators are also close together, but their values lie 3 orders of magnitude below the limit provided by the Debye equation.[12] The rate constant for the reaction between $HDNSA^-$ and OH^- is also much below the diffusional limit, but definitely higher then the specific rates for proton transfer from $HDNSA^-$ to In^{2-}. An explanation to such a difference can be found in the reduction of the electrostatic repulsion between the reaction partners when In^{2-} is replaced by OH^-. In addition, the diffusion coefficient of OH^- is certainly larger than that of the indicators. The third row of Table 2 shows that the rate constants for proton transfer from HIn^- to $DNSA^{2-}$ change by about 2 orders of magnitude, reflecting the variation of the indicator pK.

The reduction of reactivity of $HDNSA^-$ (and of other salicylic acid derivatives) has been ascribed to a strong hydrogen bond at the carboxylate oxygen that hinders the transfer of the phenolic proton.[3,6] This internal H bond is also responsible for the abnormally low rate of complex formation[1,2,4,5] between protonated salicylates and metal ions as Ni^{2+}, Co^{2+}, and Zn^{2+}. Two different mechanisms can explain the behavior shown in Figure 3. The first is a two-step mechanism involving a fast preequilibrium between a *closed* and an *open* form of the salicylate monoanion followed by the step of proton transfer from the open form.[6] The second is a one-step mechanism involving direct attack by the acceptor at the closed form of the donor.[7,21] The slope of the line in Figure 3 associated to the process of proton donation to $DNSA^{2-}$ should be −1 near $\Delta pK = 0$ when the two-step mechanism is operative, whereas it should be smaller (−0.5 in the ideal case) when the one-step route is followed.[22] Our results are in favor of the two-step mechanism. In such a case, the difference of the ordinate values of the two orizontal lines in Figure 3 directly provide the value of the logarithm of the equilibrium constant for the fast step $HDNSA^-$(open) ⇔ $HDNSA^-$(closed).

This study demonstrates the usefulness of the laser detection system, especially for evaluation of multiple relaxation effects. By using conventional lamps, the fastest of the two effects could not be safely analyzed. By contrast, the signals monitored by laser, as that shown in Figure 2, are easily evaluated with small errors. In order to make a comparison of the two devices, four jumps of the same solution were performed first by the T-jump with the 50 W lamp and then by the instrument equipped with the 5 mW laser. In the former case, the standard deviations of

amplitude and relaxation time are, respectively, $\sigma_\alpha = 11\%$ and $\sigma_\lambda = 13\%$, whereas with laser monitoring the standard deviations are $\sigma_\alpha = 0.9\%$ and $\sigma_\lambda = 1.1\%$. The enhancement of the signal-to-noise ratio leads obviously to an improvement of the final results. Inspection of Table 1 shows that with BTB the standard deviation for pK_A evaluated by the dynamic method with laser detection and by the static method are similar. By contrast, in the case of TB, the dynamic method with conventional detection provides a standard deviation for pK_A about 19-fold larger than that determined by the static method.

The same considerations apply to the reaction enthalpies given in Table 3. For DNSA/BTB and DNSA/PR systems the dynamic method with laser monitoring and the static method display similar precisions, whereas for the DNSA/TB system the dynamic method with the conventional detection provides a standard deviation of $\Delta H°$ about 10-fold larger than that provided by static technique.

Finally, it is worth mentioning that the dynamic method presents the additional advantage of allowing the simultaneous evaluation of two thermodynamic parameters to be done from a relatively small number of experiments, as in the DNSA/BTB and DNSA/TB systems where reaction enthalpy and equilibrium constant have been simultaneously determined.

Appendix

The complete reaction scheme for proton transfer in aqueous medium involves R-coupled reactions, R' of which being thermodynamically independent.

$$L^{2-} + H^+ \rightleftharpoons HL^- \tag{A1}$$

$$HL^- + In^{2-} \rightleftharpoons L^{2-} + HIn^- \tag{A2}$$

$$HIn^- + OH^- \rightleftharpoons In^{2-} + H_2O \tag{A3}$$

$$In^{2-} + H^+ \rightleftharpoons HIn^- \tag{A4}$$

$$H^+ + OH^- \rightleftharpoons H_2O \tag{A5}$$

$$HL^- + OH^- \rightleftharpoons L^{2-} + H_2O \tag{A6}$$

If the kinetically elementary steps (A1−A3) are chosen as the thermodynamically independent ones, then the remaining reactions are obtained by linear combinations of them. Namely, A4 = A1 + A2, A5 = A1 + A2 + A3, and A6 = A2 + A3.

The kinetic behavior of the system can be expressed in matrix form by eq A7

$$-\boldsymbol{\zeta} = \mathbf{rg}\boldsymbol{\zeta} \tag{A7}$$

where **r** is a diagonal matrix whose elements are the exchange rates of the six reactions (A1−A6) and **g** is a 6 × 6 symmetric matrix whose elements are defined according to the Castellan's paper.[23] $\boldsymbol{\zeta}$ is a column vector whose elements indicate the extent of reaction of the six elementary steps.

We shall present here a method that allows an easy derivation of the set of equations describing the kinetic a thermodynamic behavior of the system. We shall make use of a "stoichiometric" $R' \times R$ matrix, $\boldsymbol{\nu}$, whose column elements indicate the factor by which each of the independent steps should be multiplied before making the linear combinations that express any of the elementary reactions in terms of the thermodynamically independent steps. In our case, the matrix $\boldsymbol{\nu}$ reads

$$\boldsymbol{\nu} \equiv \begin{pmatrix} 1 & 0 & 0 & 1 & 1 & 0 \\ 0 & 1 & 0 & 1 & 1 & 1 \\ 0 & 0 & 1 & 0 & 1 & 1 \end{pmatrix} \tag{A8}$$

Equation A7 can be rewritten as

$$-\boldsymbol{\zeta} = \mathbf{rg}'\boldsymbol{\xi} \tag{A9}$$

where $\mathbf{g}'$ is a rectangular $R \times R'$ (in our case 6 × 3) matrix made by the first three columns of **g** whereas $\boldsymbol{\xi}$ is a column vector whose elements are given by eq A10.

$$\xi_k = \sum_{m=1}^{R} \nu_{km}\zeta_m \qquad k = 1...R' \tag{A10}$$

Premultiplying both members of eq A9 by the matrix $\boldsymbol{\nu}$, one obtains the reduced set of equations A11.

$$-\boldsymbol{\xi} = \mathbf{B}\boldsymbol{\xi} \tag{A11}$$

The elements b_{jk} of the $R' \times R'$ (in our case 3 × 3) matrix **B** include the contributions to the overall rate of the independent *and* of the dependent steps. They are evaluated by eq A12

$$b_{kj} = \sum_{m=1}^{R} \nu_{km}\mathbf{r}_m\mathbf{g}_{mj} \qquad k = 1...R' \tag{A12}$$

$$j = 1...R'$$

Once the elements of **B** have been found, the dynamical behavior of the system can be easily described by solving the eigenvalue problem, which leads to the system of homogeneous linear equations (A13).

$$(\mathbf{B} - \lambda_k\mathbf{I})\mathbf{C} = 0 \tag{A13}$$

The eigenvalues, λ_k, of the matrix **B** coincide with the reciprocal relaxation times. **I** is the identity matrix, whereas **C** are column vectors associated to λ_k. A nontrivial solution to eq A13 exists only if the determinant of the matrix $(\mathbf{B} - \lambda_k\mathbf{I})$ is zero. Our system is characterized by three eigenvalues, then:

$$|\mathbf{B} - \lambda\mathbf{I}| = \begin{vmatrix} b_{11} - \lambda & b_{12} & b_{13} \\ b_{21} & b_{22} - \lambda & b_{23} \\ b_{31} & b_{32} & b_{33} - \lambda \end{vmatrix} = 0 \tag{A14}$$

The experimental relaxation times and eq A14 were used to evaluate the rate constants of the reacting systems through a nonlinear least-squares analysis.[9] Hence, the elements C_{jk} of the eigenvectors **C** were evaluated with the help of eq A13. Each element C_{jk} is a concentration-dependent quantity that multiplies the jth elementary step in the linear combination leading to the kth normal reaction. After division of all terms by C_{3k}, the three normal reactions will read

$$(C_{1k}/C_{3k})\mathrm{A1} + (C_{2k}/C_{3k})\mathrm{A2} + \mathrm{A3} \qquad k = 1, 2, 3 \tag{A15}$$

The thermodynamic parameters of the normal reactions are evaluated by the analysis of the relaxation amplitudes, and finally, through their dependence on the coefficients C_{jk}, the thermodynamic parameters of the individual steps are obtained.

Acknowledgment. The authors are indebted to Prof. H. J. G. Hayman of The Hebrew University of Jerusalem for valuable discussions and helpful suggestions.

References and Notes

(1) Mentasti, E.; Pellizzetti, E.; Secco, F.; Venturini, M. *Inorg. Chem.* **1979**, *18*, 2007.
(2) Mentasti, E.; Secco, F.; Venturini, M. *Inorg. Chem.* **1980**, *19*, 3528.
(3) Diebler, H.; Secco, F.; Venturini, M. *J. Phys. Chem.* **1984**, *88*, 4229.
(4) Diebler, H.; Secco, F.; Venturini, M. *J. Phys. Chem.* **1987**, *91*, 5106.
(5) Diebler, H.; Secco, F.; Venturini, M. *J. Phys. Chem.* **1989**, *93*, 1691.
(6) Eigen, M.; De Mayer, L. In *Techniques of Organic Chemistry*, 2nd ed.; Weissberger, A., Ed.; Wiley: New York, 1963; Vol. VIII, Part 2.
(7) Perlmutter-Hayman, B.; Shinar, R. *Int. J. Chem. Kinet.* **1978,** *10*, 407.
(8) Citi, M.; Festa, C.; Secco, F.; Venturini, M. *Instr. Sci. Technol.* **1995**, *23*, 191.
(9) Provencher, S. W. *J. Chem. Phys.* **1976**, *64*, 2772.
(10) Meites, L. *The General Non-linear regression Program CFT4A*; The George Mason Institute: Fairfax, VA, 1985; p 218.
(11) Eigen, M. *Angew. Chem., Int. Ed. Engl.* **1964**, *3*, 1.
(12) Debye, P. *Trans. Electrochem. Soc.* **1942**, *82*, 265.
(13) Prue, J. E. *Ionic Equilibria, The International Encyclopedia of Physical Chemistry and Chemical Physics*; Pergamon Press: Oxford, 1966; Topic 15, Vol. 3, p 36.
(14) Smith, R. M.; Martell, A. E. *Critical Stability Constants*; Plenum: New York, 1976; Vol. IV.
(15) Perlmutter-Hayman, B.; Shinar, R. *Isr. J. Chem.* **1975**, *13*, 137.
(16) Citi, M.; Secco, F.; Venturini, M. *J. Chem. Phys.* **1988**, *92*, 6399.
(17) Secco, F.; Venturini, M. *J. Chem. Soc., Faraday Trans.* **1993**, *89*, 719.
(18) Secco, F.; Venturini, M.; Fanelli, N. *J. Solut. Chem.* **1994**, *23*, 483.
(19) Secco, F.; Venturini, M. *J. Thermal Anal.* **1994**, *41*, 1659.
(20) Bishop, E. *Indicators*; Pergamon Press: Oxford, 1972; p 65.
(21) Miles, M. H.; Eyring, E. M.; Epstein, W. W.; Ostlund, R. E. *J. Phys. Chem.* **1965**, 69, 467.
(22) Hibbert, F. *Acc. Chem. Res.* **1984**, *17*, 115.
(23) Castellan, G. W. *Ber. Bunsen-Ges. Phys. Chem.* **1963**, *67*, 898.